SLOTTED CIRCULAR PATCH MIMO ANTENNAS FOR MULTIBAND AND UWB APPLICATIONS

Muvvala Kalpana[1] and R. Ramana Reddy[2]
[1]JNTUK, Andhra Pradesh, India
[2]JNTUACEK, Kalikiri, Andhra Pradesh, India
E-Mail: muvvala.kalpana@gmail.com

ABSTRACT

In this paper, a defective ground structure (DGS) based 2-port and 4-port circular patch antennas with rectangular slots (CPRS) is presented. The proposed CPRS MIMO antenna with quadrilateral DGS delivers ultra-wide bandwidth (UWB) and multiband frequencies. The 40mm x 40mm x 1.6mm CPRS MIMO antenna operates in the frequency band of 4 GHz to 20 GHz. The 4-port CPRS MIMO antenna uses three frequency bands for operation with a bandwidth of 360MHz, 1.21GHz, and 1.15GHz. With the introduction of DGS, the bandwidth increases to 3.44 GHz, 2.01 GHz, and 5.73 GHz, and peak gain is increased to 6.9 db. Other performance characteristics observed are ECC < 0.04, DG > 9.99, TARC is -27.5 dB, and CCL < 0.275 bits/Hz/sec. Simulations are performed in ANSYS HFSS EM solver.

Keywords: circular patch, slots, MIMO, UWB, DGS, multiband.

Manuscript Received 27 October 2024; Revised 24 December 2024; Published 25 January 2025

1. INTRODUCTION

The developments in wireless communication devices are contributing to a rise in demand for low-profile, compact antennas that possess an enormous operating frequency bandwidth as well as significant gain. For such applications, microstrip patch antennas have numerous benefits, such as low profile, lightweight, and compactness. The demand for wireless networks with higher data rates and channel capacities has increased due to the extensive use of online platforms. MIMO-printed antennas have thereby become a viable option for high-speed communication technologies, representing a novel form of antenna design.

A four-element MIMO antenna resonates at three frequency bands from 3.3GHz - 3.7GHz, 5.15GHz - 5.87GHz, and 7.1GHz - 7.9GHz is achieved by various slots on square-shaped antenna elements along with a mutual coupling of < -22 dB and gain ranging between 1.4 - 4.6 dBi is reported [1]. A quasi-complimentary antenna for a MIMO system has a gain of 2.8 dB at 2 GHz and 5.7 dB at 5 GHz and operates in a frequency spectrum of 0.7 to 2.1 GHz with envelope correlation < 0.04% [2]. MIMO antenna with two microstrip fed antenna elements and a T-shaped strip, operating in a 3.08GHz - 11.8GHz frequency band with a rejection band of 5.03GHz - 5.97GHz, -15 dB of isolation and 0.02 of ECC is presented [3]. An empirical approach for calculating different DRA modes is discussed with new ideas for hybrid DRA designs [4].
Two elements MIMO antenna with a T junction power feed network operating over a frequency band of 25.5GHz - 29.6GHz with 8.3dBi gain is reported [5]. Two meandered monopole-based MIMO antennas with L-shaped parasitic strips and stubs are reported with high isolation [6]. MIMO antenna contains two L slot elements suitable for UWB applications with an ECC of 0.02 is presented [7]. A 42 x 25 mm^2 MIMO antenna operating between 3.1 to 12 GHz, ECC of 0.5, an isolation of >22 dB, and 0.4 bits/Hz/sec of CCL is reported [8]. Two rectangular dielectric resonator MIMO antennas with microstrip fed slots resonate at a frequency band of 27.25 to 28.59 GHz with an isolation of 24dB and an ECC of 0.01 is presented [9].

To enhance isolation, a metal strip is placed on the upper surface of every dielectric resonator operating in the 34.1 to 38.9 GHz frequency region [10]. It is reported that a dual-band MIMO antenna with monopole design operates in the 2.4GHz - 2.7GHz and 3.3GHz - 3.6GHz frequency ranges [11]. An 8-port MIMO antenna operating in a 23.1 - 27.3GHz frequency band with 5.68 GHz bandwidth, a gain of 6.4 dB, and ECC < 0.03 is presented [12]. To improve isolation and obtain ECC<0.04 and DG > 7.4dB acceptable for UWB applications, an F-shaped stud is presented in the ground plane [13].

Circular slotted monopole and U-shaped monopole are used to achieve an isolation of -17dB [14]. A triple band 4-port UWB MIMO antenna with gain varying from 2.5 dBi to 5.5dBi, ECC < 0.05 and TARC < −40dB is reported [15]. A 4x6 array MIMO antenna operating in X and Ku bands with a bandwidth of 27.7 % in X-band vertical polarization is presented [16]. A hexagonal patch antenna with different slots implemented to achieve a peak gain of 6.8dBi is presented [17]. With the introduction of a pentagonal slot and DGS to the pentagonal patch antenna, the bandwidth is increased from 4.32dBi to 4.5dBi in the lower operating frequency region [18].

An asymmetry was introduced into the structure of a standard cylindrical dielectric resonator antenna to achieve two orthogonal CP radiation modes [19]. An antenna with nine dielectric resonators are proposed for X-band applications with bandwidth of 56% and 8.3 dBi of gain [20]. Rectangular slots on the octagonal patch antennas are suitable for X and Ku band applications [21].

VOL. 19, NO. 24, DECEMBER 2024 ISSN 1819-6608
ARPN Journal of Engineering and Applied Sciences

In this paper, a 2-port and 4-port CPRS MIMO antenna with and without DGS are proposed. The performance of the 4 port CPRS UWB-MIMO antenna is assessed using parametric analysis. The suggested antennas are operated for multiband and UWB applications.

The overall structure of the paper is as follows. Section 2 includes the CPRS antenna designing and modeling de. Section 3 includes a 2-Port CPRS MIMO antenna. Section 4, the performance and parametric analysis of 4 port CPRS MIMO antenna is discussed. The 2-port CPRS MIMO antenna with DGS measurement setup is presented in section 5. Section 6 compares the proposed CPRS's performance attributes. In section 7 the conclusions are presented.

2. ANTENNA MODELLING

The following steps are followed to design the CPRS antenna. At first, an antenna with the circular patch (CPA) is designed, and then a rectangular strip is integrated below the patch. After that slots are created in the CPA as shown in Figure-1.

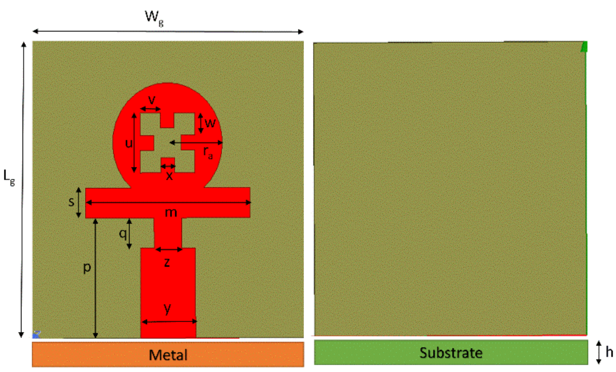

(i) (ii)

Figure-1. CPRS Antenna (i) Front View (ii) Back view.

A quadrilateral DGS implementation in the ground plane is shown in Figure-2.

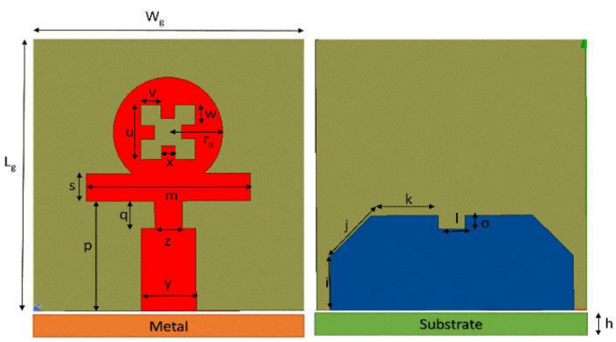

(i) (ii)

Figure-2. The CPRS Antenna with DGS (i) Front View (ii) Back view.

Table-1. The optimized dimensions of the CPRS antenna.

Parameters	Value (mm)	Parameters	Value (mm)
L_g	20	m	12
W_g	20	h	1.6
u	4	p	8
v	1.5	q	2
w	1.5	j	3
x	1	k	5
y	2	i	4
z	2	l	2
s	2	o	1

Table-1 displays the optimised CPRS antenna dimensions and the resonant frequency is calculated by the formula given below.

$$f_{reso} = \frac{8.791 \; x \; 10^9}{r\sqrt{\epsilon_r}}$$

Where

ϵ_r = Effective dielectric radius.
r = Radius of CPA.
f_{reso}= Resonant frequency of CPA.

A. Performance Analysis of Basic CPRS

In Figure-3, S_{11} plots of CPA, CPA with a rectangular strip, and CPRS are displayed. The CPA operates in 15.21 GHz to 17.91 GHz and 19 GHz to 20 GHz with 2.7 GHz and 1GHz bandwidth and a peak gain of 7.2dB. A rectangular strip is inserted into the CPA antenna and operates in the resonant band of 14.33 GHz to 17.38 GHz with a bandwidth of 3.08 GHz resonating at 11.4 GHz with 11.8 dB of gain. The CPRS antenna operates over a triple frequency band ranging from 11.02 GHz-11.37 GHz, 13.64 GHz-14.71 GHz, and 17.59 GHz–19.13 GHz with 350 MHz, 1.07 GHz, 1.54 GHz bandwidth respectively, and the gain of 6 dB.

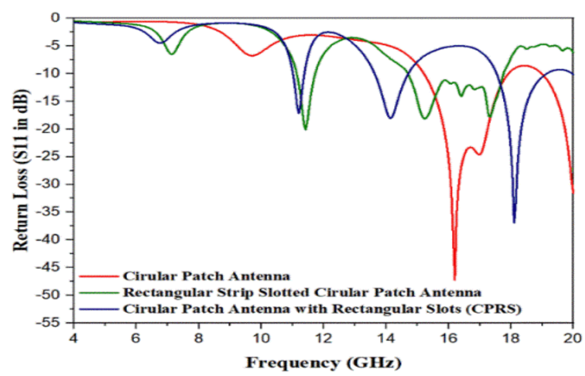

Figure-3. S_{11} plot of CPA, Rectangular strip slotted CPA and CPRS.

VOL. 19, NO. 24, DECEMBER 2024 ISSN 1819-6608
ARPN Journal of Engineering and Applied Sciences

B. Analysis of CPRS Antenna with and without DGS

The dual operating bands of the CPRS antenna with DGS range from 4.98GHz to 8.08GHz and 11.49GHz to 20GHz with a bandwidth of 3.10GHz and 8.51GHz respectively. A 6.9 dB peak gain is obtained by the antenna. The CPRS antenna without DGS offers triple frequency bands covering a bandwidth of 350 MHz, 1.07 GHz, and 1.54 GHz with a gain of 6 dB. With and without DGS, the S_{11} plots for the CPRS antenna are presented in Figure-4.

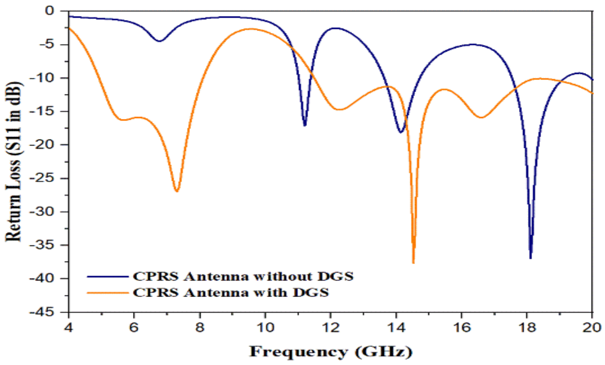

Figure-4. S_{11} plot of CPRS antenna with and without DGS.

3. 2-PORT CPRS MIMO ANTENNA

Figure-5 shows, a 2-port CPRS MIMO antenna of 40 x 20 x 1.6 mm^3.

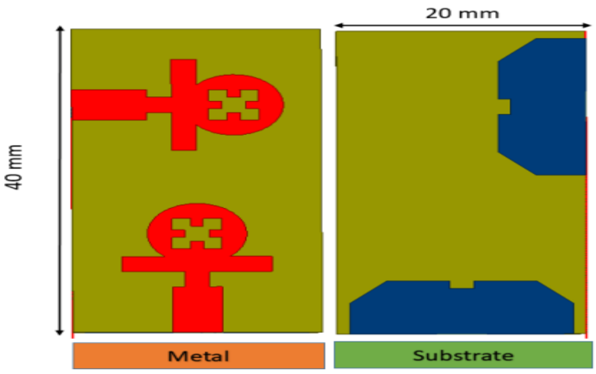

Figure-5. DGS based 2-Port CPRS MIMO antenna Front View (ii) Back view.

A. Analysis of 2-Port CPRS MIMO Antenna

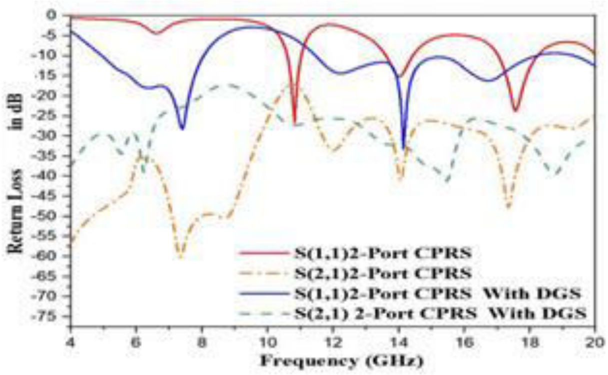

Figure-6. With and without DGS, scattering coefficients of 2-port CPRS MIMO antenna.

With and without DGS, scattering coefficients of the 2-port CPRS MIMO antenna are shown in Figure-6. The 2-port CPRS MIMO antenna without DGS offers a triple frequency band of 10.60GHz- 11.02 GHz, 13.61 GHz-14.42 GHz, and 17.03 GHz-18.22 GHz with 420 MHz, 810MHz, and 1.19 GHz of bandwidth respectively with 6.12dB of maximum gain. By introducing DGS, the antenna offers a dual frequency band of 4.96 GHz - 8.04 GHz, 11.47 GHz - 20 GHz with a bandwidth of 3.08 GHz, and 8.53GHz with a peak gain of 7.1 dB.

B. Gain

The gain of 2–port CPRS MIMO antenna without DGS varies from 4.5 dB - 6.12 dB with a maximum gain of 6.12dB at 14.02 GHz. With the introduction of DGS, the gain varies from 3.4dB to 7.1dB with a high gain of 7.1dB at 16.78GHz are shown in Figure-7.

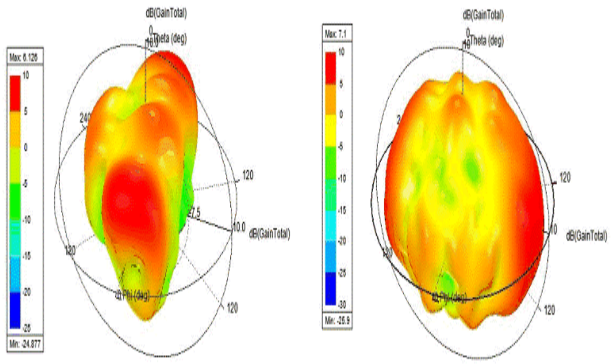

(i) (ii)

Figure-7. 3D Gain of 2-Port CPRS MIMO antenna (i) Without DGS at 14.02GHz (ii) With DGS at 16.78GHz.

C. E & H Plane Patterns

The E & H Plane patterns of the 2-port CPRS MIMO antenna are plotted at high gain frequencies without DGS at 6.26 GHz and with DGS at 10.58 GHz are presented in Figure-8.

ARPN Journal of Engineering and Applied Sciences

www.arpnjournals.com

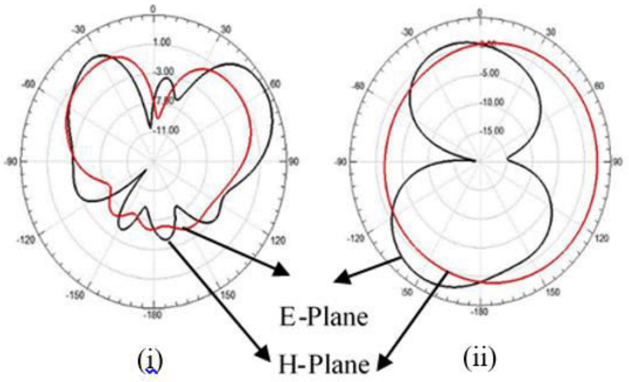

Figure-8. E & H plane patterns of 2-port CPRS MIMO antenna (i) Without DGS at 6.26GHz (ii) With DGS at 10.58GHz.

4. 4-PORT CPRS MIMO ANTENNA

The 40 x 40 x 1.6 mm^3 4-Port CPRS MIMO antenna is shown in Figure-9.

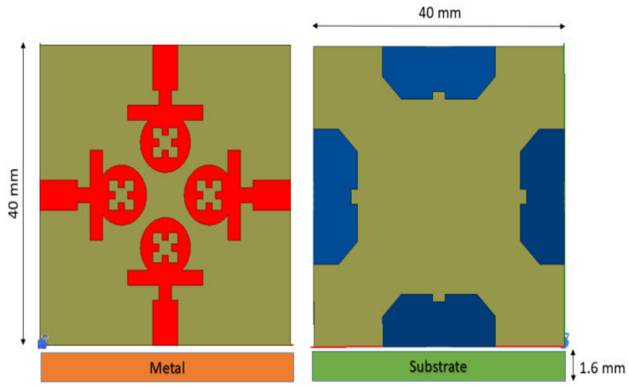

(i) (ii)

Figure-9. 4-port CPRS MIMO Antenna with DGS (i) Front View (ii) Back view.

With and without DGS, S_{11} of 4-port CPRS MIMO antenna are shown in Figure-10. Without DGS it offers triple operating bands in a frequency range of 10.96 GHz-11.32 GHz, 13.50 GHz-14.71 GHz, and 17.22 GHz-18.37 GHz with 360 MHz, 1.21 GHz, and 1.15 GHz bandwidth respectively and it offers a peak gain of 5.7dB. By introducing DGS, the antenna operated in 4.13 GHz-7.57 GHz, 11.59 GHz-13.60 GHz, and 14.27 GHz-20GHz frequency bands with 3.44GHz, 2.01GHz and 5.73GHz bandwidth respectively, and gain of 6.9 dB.

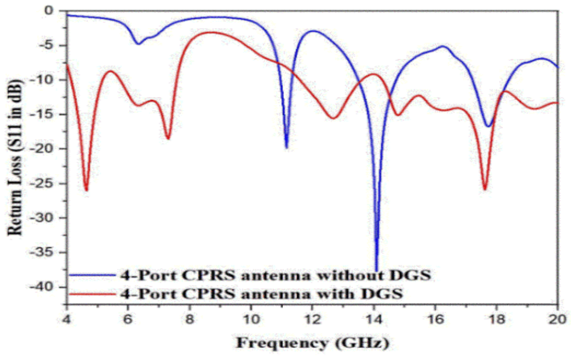

Figure-10. With and without DGS, S_{11} Plot of 4-port CPRS MIMO antenna.

The simulated parameters for characterizing the isolation of the antenna are presented in Figure-11, it shows an isolation of < -10 dB in the entire frequency band, and the parameters of S_{21} and S_{41} are observed to be symmetrically equal.

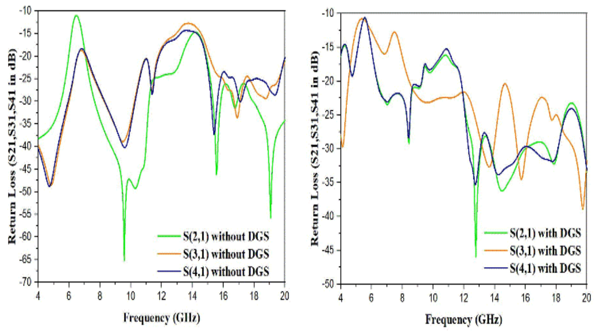

(i) (ii)

Figure-11. S- parameters of 4-port CPRS MIMO antenna (i) Without DGS (ii) With DGS.

A. 3D Gain

The gain of a 4-port CPRS MIMO antenna without DGS varies from 3.8 dB to 5.7 dB with a gain of 5.7 dB at 14.02 GHz. With the introduction of DGS, the gain varies from 3.1 to 6.9 dB with a peak gain of 6.9 dB at 16.2 GHz are shown in Figure-12.

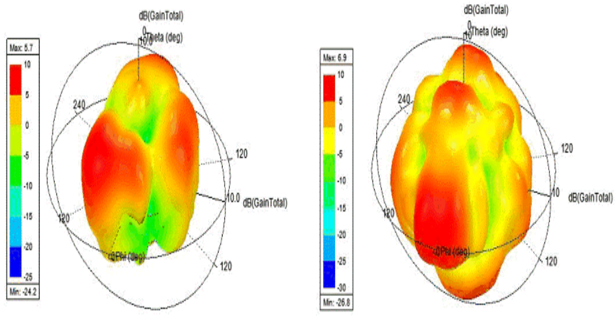

(i) (ii)

Figure-12. 3D Gain of 4-Port CPRS MIMO antenna (i)Without DGS (ii) With DGS.

ARPN Journal of Engineering and Applied Sciences

B. E & H Plane Patterns

The E & H Plane patterns of the 4-port CPRS MIMO antenna are shown in Figure-13.

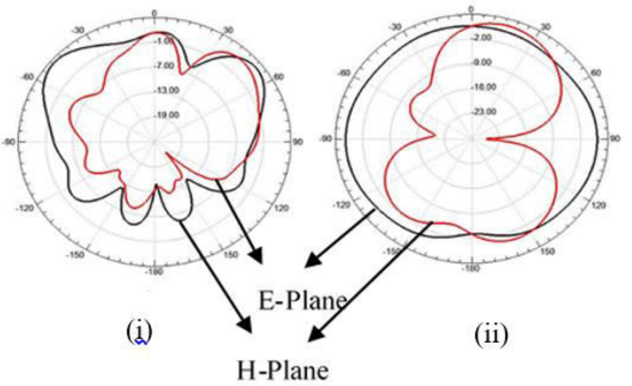

Figure-13. E & H plane patterns of 4-port CPRS MIMO antenna (i) Without DGS at 7.29GHz (ii) With DGS at 4.08GHz.

C. Parametric Analysis of 4-Port CPRS MIMO Antenna

In the section below, the parametric analysis of the 4-port CPRS MIMO antenna is presented.

a) Envelope correlation coefficient (ECC)

The ECC provides information on the radiation patterns of the two separate antennas. Isolation can also be studied from the Envelope Correlation Co-efficient (ECC). The ideal value for ECC is zero, in practice, the acceptable limit must be less than 0.5. Figure-14 shows ECC for the proposed 4-port CPRS MIMO antenna is less than 0.04.

$$\mathrm{ECC} = \frac{(S_{ii}{}^{*}S_{ij} + S_{ji}{}^{*}S_{jj})^2}{(1 - |S_{ii}|^2 - S_{ij}{}^2)(1 - |S_{ij}|^2 - S_{Jj}{}^2)}$$

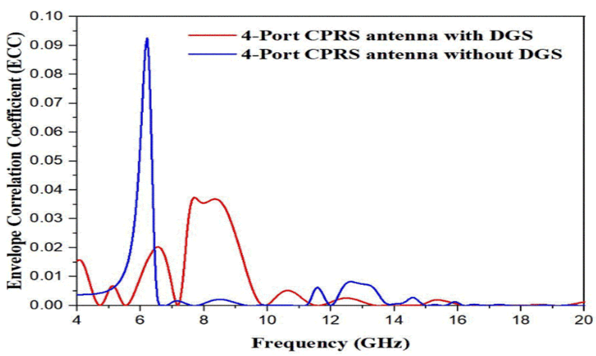

Figure-14. ECC of 4-Port CPRS MIMO antenna with and Without DGS.

b) Diversity gain (DG)

Figure-15 illustrates the 4-port CPRS MIMO antenna's DG, which ranges between 9.99 to 10 dB across the band.

$$DG = 10\sqrt{1 - |\rho_{eij}|^2}$$

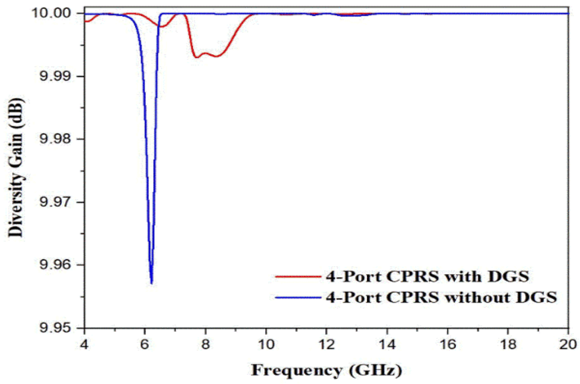

Figure-15. DG of 4-Port CPRS MIMO antenna with and without DGS.

c) Total active reflective coefficient (TARC)

A parameter to consider when describing multiport arrays of antennas used in MIMO platforms and array antennas is the TARC and it is calculated by the given formula. Figure-16 shows the TARC values. The lowest value of -27.5 dB TARC is obtained.

$$\Gamma = \frac{\sqrt{\left(|S_{ii} + S_{ij}e^{j\theta}|^2\right) + \left(|S_{ji} + S_{jj}e^{j\theta}|^2\right)}}{\sqrt{2}}$$

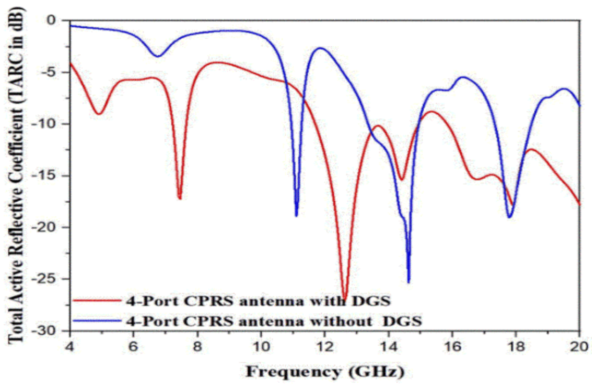

Figure-16. TARC of 4-Port CPRS MIMO antenna With and without DGS.

d) CCL

The CCL is the channel capacity loss due to correlation. By using the given formula, the CCL obtained is < 0.4 bits/Hz for the total operating band and it varies from -0.1 to 0.275 bits/Hz/sec as shown in Figure-17.

$C_{loss} = -log_2 \det(a)$

Where 'a' is the correlation matrix

$$a = \begin{bmatrix} c_{11} & c_{12} \\ c_{21} & c_{22} \end{bmatrix}$$

Where,

$c_{xx} = 1 - (|S_{xx}|^2 - |S_{xy}|^2)$

$c_{xy} = (S_{xx}{}^{*}S_{xy} + S_{yx}S_{yy}{}^{*})$

$c_{yx} = (S_{yy}{}^{*}S_{yx} + S_{xy}S_{xx}{}^{*})$

$c_{yy} = 1 - (|S_{yy}|^2 - |S_{yx}|^2)$

 ISSN 1819-6608
ARPN Journal of Engineering and Applied Sciences

www.arpnjournals.com

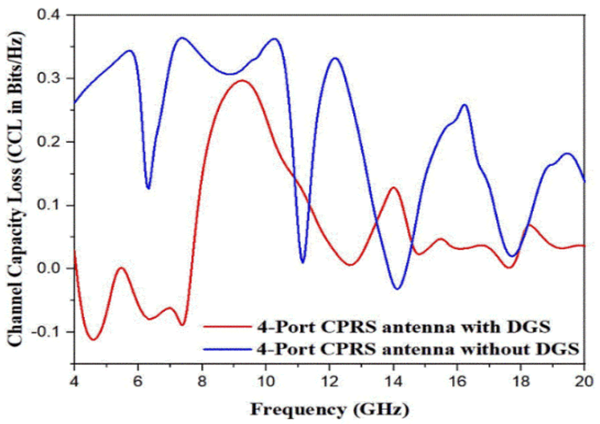

Figure-17. CCL of 4-Port CPRS MIMO antenna with and without DGS.

5. FABRICATION AND MEASUREMENT OF 2-PORT MIMO WITH DGS

Figure-18 shows the fabricated structure of a 2-port MIMO antenna with DGS. Figure-19 shows the experimental setup in an anechoic chamber. In Figure-20 the comparison of measured and simulated S11 is presented. Figure-21 shows the normalised measured E & H plane patterns.

(i) (ii)

Figure-18. Fabricated structure of 2-port MIMO antenna with DGS (i) Front view (ii) Back view.

(i) (ii)

Figure-19. Experimental setup of 2-port MIMO antenna with DGS.

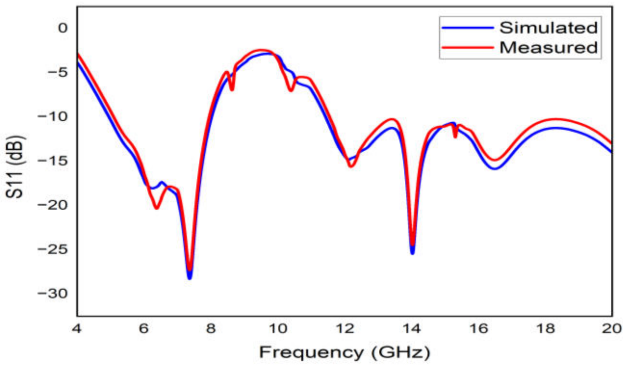

Figure-20. Reflection Coefficient (S_{11}) of simulated and measured values comparison of 2-port MIMO antenna with DGS.

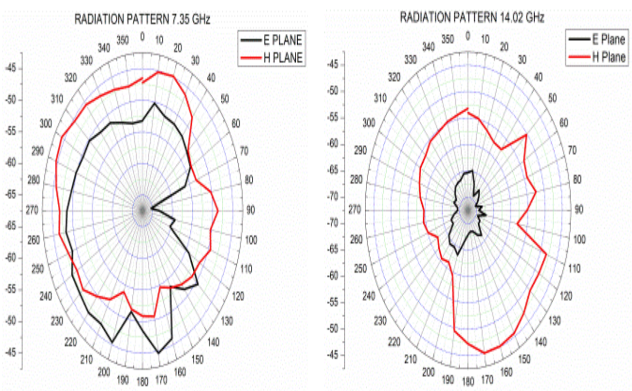

(i) (ii)

Figure-21. E & H plane patterns of 2-port MIMO antenna with DGS (i) at 7.35 GHz (ii) at 14.02 GHz.

6. COMPARISON OF PERFORMANCE CHARACTERISTICS OF THE PROPOSED ANTENNAS

The comparison of performance characteristics of the CPRS, 2-port, and 4-port CPRS MIMO antennas with and without DGS are tabulated in Table-2.

Table-2. Comparison of the suggested antenna structures simulated outcomes.

Type of Antenna	Bandwidth (GHz)	Operating frequencies (GHz)	Peak Gain (dB)
CPRS Antenna	0.35 1.07 1.54	(11.02 - 11.37), (13.64 - 14.71), (17.59 - 19.13)	6
CPRS Antenna with DGS	3.10 8.51	(4.98 - 8.08), (11.49 - 20)	6.9
2-Port CPRS Antenna	0.42 0.81 1.19	(10.60 - 11.02), (13.61 - 14.42), (17.03 - 18.22)	6.126
2-Port CPRS Antenna with DGS	3.08 8.53	(4.96-8.04), (11.47-20)	7.1
4-Port CPRS Antenna	0.36 1.21 1.15	(10.96 - 11.32), (13.50 - 14.71), (17.22 - 18.37)	5.7
4-Port CPRS Antenna with DGS	3.44 2.01 5.73	(4.13 – 7.57), (11.59 – 13.60), (14.27 – 20)	6.9

Table-3. Comparison of the works reported in open literature.

Ref.	Size (mm^2)	Operating frequency (GHz)	10dB RL BW (GHz)	Gain (dB)
[1]	39 x 39	3.3-3.7, 5.15-5.87, 7.1-7.9	0.4, 0.72, 0.8	1.4-4.6
[5]	30 -35	26.8-29.6	2.8	8.3
[7]	42 x 25	3.1-12	8.9	1.7-4.2
[11]	31.2x31.2	23.1-27.3	5.68	6.4
[15]	77 x79	8.3-11.3, 12.2-15.52	3.0, 3.32	2.5-5.5
[17]	52 x46	2-13.5	11.5	6.8
[18]	52 x46	2.2-4.7, 7.1-10.4	2.5, 3.3	4.32
CPRS	20 x20	4.98-8.08, 11.49-20	3.10, 8.53	6.9
2-port CPRS MIMO	40 x20	4.96-8.04, 11.47-18.75	3.08 7.28	7.1
4-port CPRS MIMO	40 x40	4.13-7.57, 11.59-13.60, 14.27-20	3.44, 2.01, 5.73	6.9

7. CONCLUSION

The proposed CPRS MIMO antennas are designed for multiband and UWB applications. The 2-port CPRS MIMO antenna with DGS is fabricated which operates over a frequency range of 4.96 - 8.04GHz and 11.47 - 20GHz. With the introduction of DGS, the operating bandwidth and peak gain are increased. The 2-port CPRS MIMO antenna is a broadband antenna with a bandwidth ratio of 53.9% and it is operated in C, Ku, and Ka bands. The 4-port CPRS MIMO antenna is a multiband antenna with a bandwidth of 360MHz, 1.21GHz, and 1.15GHz with a peak gain of 5.7dB. With the introduction of quadrilateral DGS the operating frequency bandwidths are increased to 3.44 GHz, 2.01 GHz, and 5.73 GHz respectively with a peak gain of 6.9 dB. The performance characteristics of the proposed antenna are ECC < 0.04, DG > 9.99dB, TARC is -27.5 dB, and CCL < 0.275 bits/Hz/sec. Measured and simulation results are in close agreement.

REFERENCES

[1] Tang Z., Wu X., Zhan J., Hu S., Xi Z. and Liu Y. 2019. Compact UWB-MIMO Antenna with High Isolation and Triple Band-Notched Characteristics. IEEE Access. 7: 19856-19865.

[2] S. M., Eva. A. D., Fabres. M. C., Ferrando-. B. M. and Salonen. E. T. 2012. Improved Planar Wideband Antenna Element and its usage in a Mobile MIMO System. IEEE Antennas and Wireless Propagation Letters. 11: 826-829.

[3] Kang Le, Hui Li, X. Wang and Shi X. 2015. Compact Offset Microstrip-Fed MIMO Antenna for Band-Notched UWB Applications. IEEE Antennas and Wireless Propagation. Letters. 14: 1754-1757.

[4] Rajasekhar N., Darimireddy N. K., Kumari R., Chan-Wang Park and R. R. Reddy. 2021. Circularly Polarized Hybrid Dielectric Resonator Antennas: A Brief Review and Perspective Analysis. Sensors, 21, 4100; https://doi.org/10.3390/s21124100

[5] M. K. Iffat, S. N. Hussain, N. Rahman, M. Fawad, S. Sajid, M. M. Jamil. K. and Amin Y. 2020. 4-Port MIMO Antenna with Defected Ground Structure for 5G Millimeter Wave Applications. Electronics. 9(1): 71.

[6] Deng J. Ya, Guo Li-X. and Long X. L. 2016. An Ultra-wideband MIMO Antenna with a High Isolation. IEEE Antennas and Wireless Propagation. Letters. 15, 182-185.

[7] Jain R., Hu W., Yingzeng Y. and F. R. 2014. Compact Printed MIMO Antenna for UWB Applications. IEEE Antennas and Wireless Propagation. Letters. 13: 1517-1520.

[8] Gunjan S. and M. A. 2016. Compact MIMO Slot Antenna for UWB Applications. IEEE Antennas and Wireless Propagation. Letters. 15, 1057-1060.

[9] Z. Y., D. J., Li. M., Sun. D. and Guo Li-Xin. 2019. A MIMO Dielectric Resonator Antenna with Improved Isolation for 5G mm-Wave Applications. IEEE Antennas and Wireless Propagation. Letters. 18(4): 747-751.

[10] K. J. Wang, K. H. G. and Eibert F. T. 2017. A mm-Wave Patch Antenna with Broad Bandwidth and a Wide Angular Range. IEEE Transactions. On Antennas and Propagation. 65(8): 4293-4298.

[11] J. W., Cui. Y., L. B., Wei. H. and Xi. Y. 2019. A Dual-Band MIMO Antenna with Enhanced Isolation for 5G Smartphone Applications. IEEE Access. 7: 112554-112563.

[12] S. N. Shoaib, S. Khattak, Y. R. Shoaib, I. Ch. X. and Aqib P. 2018. MIMO Antennas for Smart 5G Devices. IEEE Access. 6: 77014-77021.

[13] I. A. Omar, A. S. Arbab, W. A. and B. S. 2018. Mutual Coupling Reduction Using F-Shaped Stubs in UWB-MIMO Antenna. IEEE Access. 6, 2755-2759.

[14] K. Saheed. M., Adnan I. A., Sajid M. A., Antonio D. C. and Braaten B. D. 2015. A compact four elements UWB MIMO antenna with on-demand WLAN rejection. Microwave and Optical Tech. Lett. 58(2): 270-276.

[15] Zhijian Ch, Weisi Z. and Jingsong H. 2021. A Miniaturized MIMO Antenna with Triple Band-Notched Characteristics for UWB Applications. IEEE Access. 9: 63646-63655.

[16] Lingyu K. and Xiaojian Xu. A. 2018. Compact Dual-Band Dual-Polarized Microstrip Antenna Array for MIMO-SAR Applications. IEEE Transactions. Antennas and Propagation. 66(5): 2374-2381.

[17] Kalpana Muvvala, Ramana Reddy R. & Naresh Kumar. D. 2017. Design and Analysis of Various Slots on Hexagonal Boundary Patch Antennas for Enhanced Gain. Lecture Notes in Electrical Engineering. 63-71.

[18] Kalpana M. and Ramana Reddy R. 2017. Analysis of the impact of slot and DGS on bandwidth & gain of a pentagon patch antenna. 2017 IEEE International Conference on Antenna Innovations & Modern Technologies for Ground, Aircraft and Satellite Applications, IAIM, pp. 1-5.

[19] Kalpana M. and Ramana Reddy R. 2022. Circularly Polarized Split Cylindrical Dielectric Antenna for Wireless Applications. IEEE Wireless Antenna and Microwave Symposium, WAMS.

[20] Runa K. and Behera S. K. 2013. Nine-element frequency independent dielectric resonator array for X-band applications. Microwave and Optical Technology Letters. 55(2): 400-403.

[21] Lakshmi V. A., Kalpana M., Reddy R. R. and S. R. Chowdary P. 2023. A Slotted Octagonal Patch Antenna for Multi-Band and High Gain Applications. IEEE Wireless Antenna and Microwave Symposium (WAMS).